

Molecular weight dependence of the tracer diffusion coefficient of short chains in the microphase domain of block copolymers as studied by the pulsed-field gradient nuclear magnetic resonance method*

J. Baba, T. Kubo, A. Takano and T. Nose†

Department of Polymer Chemistry, Tokyo Institute of Technology, 2-12-1 Ookayama, Meguro-ku, Tokyo 152, Japan

(Received 17 February 1993; revised 15 April 1993)

By means of the pulsed-field gradient nuclear magnetic resonance method, the tracer diffusion of homopolymer chains dissolved in the microphase domain of block copolymer mesophase has been studied for two systems: poly(dimethylsiloxane) (PDMS) in polystyrene(PS)-*b*-PDMS in the presence of *d*₆-benzene as a plasticizer, and poly(ethylene glycol) (PEG) in PS-*b*-poly(hydroxystyrene-*g*-PEG)-*b*-PS. Comparing the diffusion coefficient *D* of the tracers in the block copolymer matrices with the self-diffusion coefficient *D*_s of the pure tracers, two regimes with a different dependence of *D*/*D*_s on the molecular weight *M* of the tracers have commonly been found in the two systems. In the lower *M* regime (regime I), the ratio *D*/*D*_s increased remarkably with increasing *M*, whereas in the higher *M* regime (regime II), the value of *D*/*D*_s was ~0.15 and was independent of *M*. This behaviour could be explained by the *M* dependence of the spatial distribution of the tracer chains in the microphase domain. In regime I, the tracers deeply penetrate into the brushes of the PDMS or grafted PEG with the depth decreasing with increasing *M*, while in regime II the tracer chains do not penetrate well into the PDMS or PEG brushes, but rather are interposed between the layers.

(Keywords: chain diffusion; block copolymers; microphase structure)

INTRODUCTION

The diffusion behaviour of polymer chains strongly depends upon structure and mobility of the environment as well as on the chain length of the polymer. Chain diffusion in ordinary polymeric systems such as dilute solutions, semidilute solutions and melts have been extensively studied both experimentally and theoretically^{1,2}. In these studies, entanglements and hydrodynamic interactions have been the main issues. More heterogeneous matrices such as porous glasses and membranes, and the mesophase of branched polymers and block copolymers in the presence of solvent or no solvent can also be studied. Recently, chain diffusion in these heterogeneous matrices has received a lot of attention. The diffusion in porous media has been investigated by dynamic light scattering³⁻⁶ and forced Rayleigh scattering⁷, and discussed on the basis of various theoretical treatments⁸⁻¹¹. The permeability of polymer chains through porous membranes has also been studied experimentally and theoretically in terms of inhomogeneity of the channel size in the membranes^{12,13}. In macroscopic tracer diffusion and the permeability of polymer chains through such heterogeneous matrices, the spatial distribution of the chains in the matrices can play

an important role as well as hydrodynamics and chain motion in a confined space.

Another interesting example of diffusion in heterogeneous matrices, which will be dealt with in this paper, is the diffusion of chains dissolved in microphases formed by block copolymers. This is quite interesting and important from both technological and scientific view points. Recently, Balsara *et al.*¹⁴ measured the diffusion coefficient of tracer chains in microstructured block copolymer solutions by means of forced Rayleigh scattering, and found a slowing down of the diffusion in the microstructure compared with that in homogeneous solution. A theoretical treatment of chain diffusion in microstructured block copolymers has been proposed by Fredrickson and Milner¹⁵. In this case, the spatial distribution of the tracer chain (partition effects) may be an important factor for determining the diffusion coefficient.

In our study, the tracer diffusion coefficient of linear homopolymer chains dissolved in microphase domains of block copolymers was measured by means of pulsed-field gradient (PFG) n.m.r. The tracer chains were confined in brushes of matrix chains which are attached on the other layer at their ends. Two types of block copolymers were chosen: one was a diblock copolymer, and the other was a triblock copolymer with many grafted branches on the middle block. The dissolved tracer chains were of the same chemical species as one of the blocks for the diblock copolymer, and the same as

* This work was partly reported in *Rept Prog. Polym. Phys. Jpn* 1991, **34**, 153

† To whom correspondence should be addressed

the grafted chains for the triblock copolymer. Here, particular attention is focused on the dependence of the diffusion on the molecular weight of the tracer chain, because the characteristic behaviour of the diffusion in the microstructured block copolymer must reflect the molecular weight dependence of the tracer diffusion. In fact, tracer diffusion has a very unique molecular weight dependence. It will be demonstrated that PFG n.m.r. can be a useful tool for measuring the tracer diffusion coefficient in complex systems with no artificial labelling.

EXPERIMENTAL

Materials

The diblock copolymer was a polystyrene-*b*-poly(dimethylsiloxane) (PS-*b*-PDMS) synthesized by anionic polymerization. The molecular weights (M_n) of the PS and PDMS blocks were determined by vapour pressure osmometry (v.p.o.) and n.m.r. spectroscopy to be 8100 and 6900, respectively, and the polydispersity index (M_w/M_n) determined by gel permeation chromatography (g.p.c.) was 1.39. Low molecular weight PDMS was obtained from Shin-etsu Chemical Co. (KF-96H). High molecular weight PDMS was anionically polymerized. The M_n values determined by v.p.o. ranged from 460 to 6500, and the polydispersity indices evaluated by g.p.c. were within the range of $1.09 < M_w/M_n < 1.1$ for all samples, but the lowest molecular weight PDMS with $M_n = 460$ was virtually monodisperse, i.e. the pentamer.

The triblock copolymer was a PS-*b*-poly(hydroxystyrene-*g*-poly(ethylene glycol))-*b*-PS [PS-*b*-P(S-*g*-PEG)-PS]. The M_w s of the PS blocks were 47 000 and 50 000, respectively, the M_w of the PS backbone in the P(S-*g*-PEG) blocks was 31 000, and the M_w and number of grafted PEG were 290 and 130, respectively. The molecular weight distribution of the sample was reasonably narrow¹⁶. Linear PEGs for the tracer were obtained from Wako-Junyaku Industrial Co. and Tokyo-Kasei Industrial Co., and were used as received. The nominal molecular weights ranged from 200 to 8500. The molecular weight distribution was considered to be narrow because of the polymerization mechanism, which was supported by g.p.c. measurements ($M_w/M_n = \sim 1.1-1.2$) and by a single exponential decay of the n.m.r. signal in PFG n.m.r. measurements. Analytical grade ethylene glycol ($M_w = 62$) was used as the lowest molecular weight tracer without further purification.

Sample preparation

Compositions. System 1 is a blend of PS-*b*-PDMS and PDMS in the presence of d_6 -benzene (d_6 -Bz). Two sets (1B and 1S) were prepared. Samples of set 1B were blended by changing the molecular weight of the PDMS tracers, whilst [PDMS]/[PS-*b*-PDMS] was fixed at 10/90 (w/w). The d_6 -Bz content in a blended sample was kept at ~ 20 wt%. The d_6 -Bz was added to increase the miscibility and mobility of the blended polymers. The other set (1S) was prepared as reference samples, using PDMSs with various molecular weights in the presence of ~ 20 wt% d_6 -Bz, i.e. the same as in the blended samples.

System 2 is a blend of PS-*b*-P(S-*g*-PEG)-*b*-PS and PEG. Set 2S was for reference, consisting of pure PEG with different molecular weights. In the blended samples (2B), [PEG]/[block copolymer] was fixed at 30/70 (w/w).

Procedures. To prepare the samples of system 1 for n.m.r. measurements, PS-*b*-PDMS and PDMS samples with the desired weight ratio were homogeneously mixed in d_6 -Bz in a n.m.r. tube (5 mm in diameter), followed by removal of the solvent by evaporation at 45°C to adjust the concentration. The sample tubes were subsequently flame-sealed under mild vacuum to avoid further evaporation of the solvent. For set 2B, blended polymer samples with the desired composition were homogeneously dissolved in benzene in a n.m.r. tube, and the solvent was completely removed by evaporation. The height of the samples in the n.m.r. tube was adjusted to < 8 mm to guarantee uniformity of the magnetic field gradient.

Characterization. Morphological structures of the blended samples were characterized by small-angle X-ray scattering (SAXS) and transmission electron microscopy (TEM). Formation of the mesophase was confirmed by TEM and the diffraction ring of SAXS indicated the presence of long periods in the structure. Considering the block composition of the copolymers and the tracer concentration, the structure was most likely lamellar in both systems (sets 1B and 2B)¹⁶. No detectable orientation of the structure to the sample tube was observed by SAXS, and this was confirmed by measuring the tracer diffusion coefficient with the PFG being applied in different directions to the sample, i.e. no dependence of the diffusion coefficient on the direction was observed. Basic morphological structures may be independent of the molecular weight of tracer, because the volume fraction of the tracer was fixed.

PFG n.m.r. measurements

The n.m.r. apparatus was a JEOL GSX/GX270 with a PFG generator PFG UNIT NM-502. Two probes were used, which could generate a field gradient g up to 70 and 600 G cm⁻¹, respectively. The magnetic field gradient was calibrated by using H₂O, n-C₁₈H₃₈ and PEG ($M_w = 200$ and 400). The pulse sequence applied was of the Hahn type^{17,18} for the spin-echo technique, which has been described elsewhere¹⁹. The time interval Δ and width δ of the PFG ranged from 30 to 100 and 0.6 to 10 ms, respectively. The gradient g ranged from 60 to 600 G cm⁻¹ in the present experiments. Effects of the residual field gradient were examined according to von Meerwall and Kamat²⁰. To avoid the effect, the interval Δ was always taken to be 10 times larger than δ .

Attenuation of the echo signal A/A_0 , where A and A_0 are the intensities of echo signals with and without applying g , respectively, was analysed by the second-order cumulant expansion:

$$\ln(A/A_0) = -\bar{D}X + (\mu_2/2)X^2 \quad (1)$$

with

$$X = \gamma^2 g^2 \delta^2 (\Delta - \delta/3) \quad (2)$$

where \bar{D} is the average tracer diffusion coefficient, μ_2 is the second-moment of polydispersity of D , i.e. $\mu_2 = (D - \bar{D})^2$ and $\gamma = 2.675 \times 10^4$ s⁻¹ G⁻¹ for the proton nuclei used here. In the cases of PDMS in the presence of d_6 -Bz (set 1S), PEG in the copolymer (set 2B) and pure PEG (set 2S), the polydispersity index μ_2/\bar{D}^2 was so small that the single exponential fitting ($\mu_2 = 0$) could be applied. The signal from the grafted PEG in the blend of PEG/graft block copolymer was negligible compared

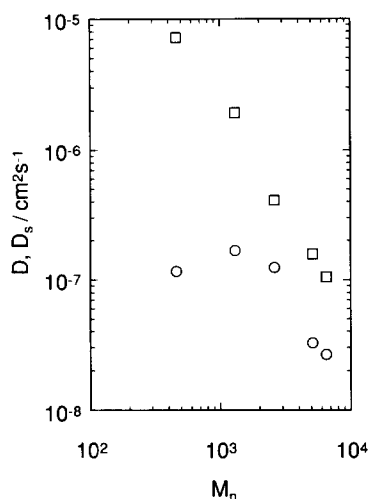


Figure 1 Dependence of the tracer diffusion coefficient of PDMS on the molecular weight (M_n) of the tracer at 30°C: (○) in PS-*b*-PDMS/PDMS/ d_6 -Bz (set 1B); (□) in the melt in the presence of 20 wt% d_6 -Bz (set 1S)

with that of the tracer PEG because of slow molecular motions. In the case of PDMS in the PS-*b*-PDMS/ d_6 -Bz, the attenuation A/A_0 did not follow the single exponential decay, but required the μ_2 term, probably owing to the presence of the signal from PDMS in PS-*b*-PDMS. The intensity of the signal from the block copolymer was very low compared with that of the tracer PDMS, which was confirmed by a very short spin-spin relaxation time of the proton nuclei in methyl groups of the block copolymer. The tracer diffusion coefficient of the block copolymer was extremely small compared with those of the tracer polymer PDMS. Considering these two facts and recalling that the \bar{D} evaluated by the cumulant method was more weighted by the faster diffusants, the \bar{D} obtained by using equation (1) was regarded as the diffusion coefficient of the tracer PDMS.

The displacement L of the tracer in the block copolymers during the time interval t of measuring the decay of the signal was of the order of 10 μm estimated by the relation $L^2 = 6Dt$. The L was much larger than the long period of the microstructure (30–45 nm), and probably even much larger than the microstructured domain size. If the domain size had been larger than L , the attenuation of the signal would have been of a non-single exponential decay, because the orientational distribution of the microstructure must directly reflect the distribution of the diffusion coefficient. In fact, there was no distribution of the diffusion coefficient, at least in the case of the PEG blends. This speculation was consistent with the morphological structure being isotropic, as mentioned before. In the sense that L was much greater than the long period and domain size, the diffusion coefficient obtained here was macroscopic.

Spin-spin relaxation time measurements

The spin-spin relaxation time T_2 of the proton nuclei for PEG of system 2 was measured by a Minispec PC-20 pulse n.m.r. spectrometer (Bruker Co. Ltd) using the Carr–Purcell–Meiboom–Gill method²¹. Attenuation of the echo signal M_y for pure PEG could be fitted to the single exponential decay function $M_y/M_{y0} = \exp(-t/T_2)$ to determine the value of T_2 , where M_{y0} is the intensity of the signal after a 90° pulse. To evaluate T_2 for the

blended system (set S2B), the attenuation was fitted by non-linear least squares fitting to the following bimodal decay function:

$$M_y/M_{y0} = f \exp(-t/T_{2a}) + (1-f) \exp(-t/T_{2b}) \quad (3)$$

where f is the proton fraction of component a , and T_{2a} and T_{2b} are T_2 values for components a and b , respectively. The faster component a ($T_{2a} > T_{2b}$) was the tracer PEG, and the slower one was the grafted PEG of the block copolymer. No signal from the PS part was detectable since segmental motions of the PS were frozen or extremely slow at the experimental temperature (80°C).

RESULTS AND DISCUSSION

Diffusion of homopolymer PDMS in the microphase domain of the PS-*b*-PDMS copolymer

In Figure 1, the tracer diffusion coefficient D of the linear homopolymer PDMS in the microstructured block copolymer (set 2B) at 30°C was plotted as a function of molecular weight of the tracer PDMS, along with the self-diffusion coefficient D_s of pure PDMS in the presence of d_6 -Bz (set 2S) for comparison. With increasing molecular weight, the tracer diffusion coefficient slightly increased initially, and then decreased parallel to D_s , while D_s decreased monotonically.

To illustrate the effects of the confinement, the ratio D/D_s was plotted against M_n (Figure 2). In the higher molecular weight range ($M_n > 2600$), referred to as regime II, the ratio D/D_s was almost constant, being ~ 0.15 . In the lower molecular weight range ($M_n < 2600$), referred to as regime I, D/D_s decreased sharply to 0.01 with decreasing molecular weight.

This characteristic molecular weight dependence can be explained by the molecular weight dependence of the spatial distribution of the tracer chains in the microdomain of the block copolymer. Figure 3 illustrates an expected spatial distribution of blended linear homopolymers in the microphase domain according to the proposal of Hashimoto *et al.*²². In regime I, where M_n of the homo PDMS is smaller than the M_n (6900) of the PDMS block of the copolymer, the homopolymer may be gradually squeezed out of the brush of PDMS chains of the block copolymers as shown in Figures 3a and b. As a result, diffusion of the tracer chain becomes faster because of fewer obstacles with increasing molecular weight of the tracer. On the other hand, in regime II, where M_n of the tracer is comparable to the M_n of the PDMS brush, the PDMS homopolymer may

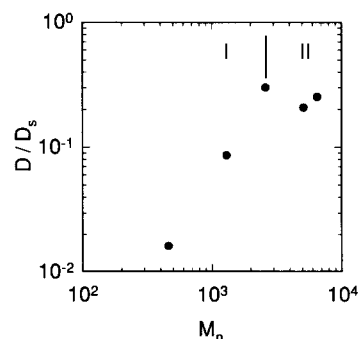


Figure 2 Dependence of the ratio D/D_s on the molecular weight (M_n) of the tracer PDMS at 30°C: (I) regime I; (II) regime II

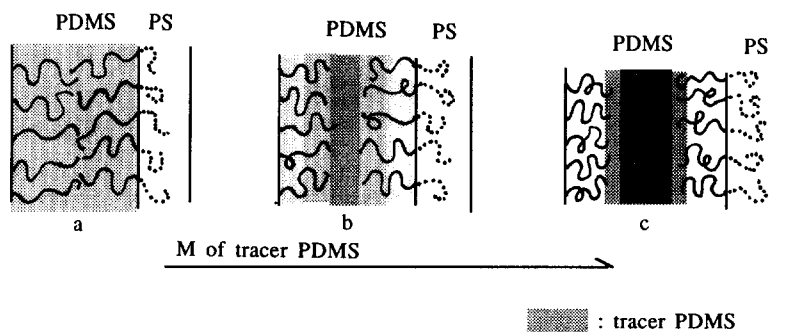


Figure 3 Schematic diagrams of the spatial distributions of homopolymer PDMS chains in microstructured PS-*b*-PDMS copolymers

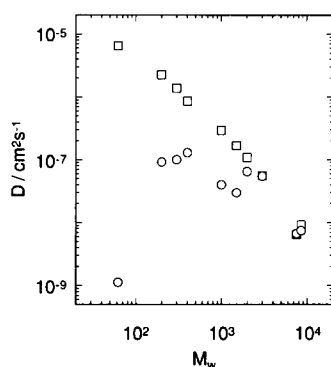


Figure 4 Dependence of the tracer diffusion coefficient of PEG on the molecular weight (M_w) of the tracer at 80°C: (○) in PS-*b*-P(S-*g*-PEG)-*b*-PS/PEG (set 2B); (□) in pure melts (set 2S)

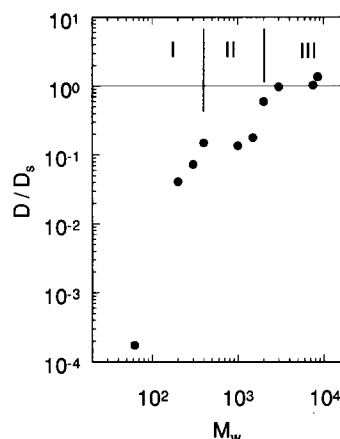


Figure 5 Dependence of the ratio D/D_s on the molecular weight (M_w) of the tracer PEG at 80°C: (I) regime I; (II) regime II; (III) regime III

be localized between the brushes, as illustrated in Figure 3c. Therefore, a decrease in mobility of segmental motions of the tracer chains owing to interposition between the microphase layers can only appear in the D/D_s behaviour, and this restriction of the segmental motions must almost be independent of the molecular weight. This is considered to be responsible for D/D_s being constant at a value of < 1 .

Diffusion of homopolymer PEG in the microphase domain of the PS-*b*-P(S-*g*-PEG)-*b*-PS copolymer

Diffusion coefficients of homopolymer PEGs in the microstructured triblock copolymer and in their pure melts are shown as a function of molecular weight of the tracer PEG in Figure 4, and the ratio D/D_s is plotted versus M_w in Figure 5. These molecular weight dependences of D and D/D_s are quite similar to those in the PDMS system, system 1. In the case of system 2, in addition to regimes I and II, one can see regime III ($M_n \geq 2000$), where the tracer diffusion coefficients of the blended samples were the same as those of the pure melts. At higher molecular weights, the tracer PEG could not be dissolved in the microphase domain and macroscopically separated from the block copolymer. This leads to the appearance of regime III. At the crossover from regime II to regime III, D changed rather abruptly. The value of D/D_s in regime II was ~ 0.12 , being almost the same as that in the PDMS system. The molecular weight around which the crossover from regime I to regime II took place was almost identical with the molecular weight of the grafted PEG (290). The tracer diffusion coefficient of the shortest tracer, ethylene

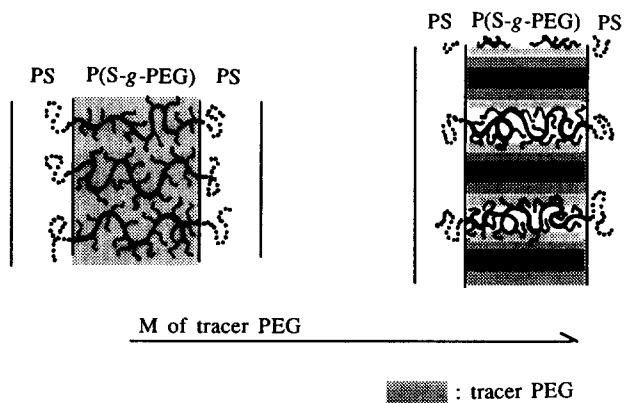


Figure 6 Schematic diagrams of the spatial distributions of homopolymer PEG chains in microstructured PS-*b*-P(S-*g*-PEG)-*b*-PS/PEG

glycol, became smaller by four orders of magnitude on being dissolved in the microdomain.

The behaviour of the tracer diffusion described above for system 2 can again be interpreted by the spatial distribution of the tracer in the microphase structure. Schematic diagrams of the spatial distribution of PEG homopolymer in the microstructured PS-*b*-P(S-*g*-PEG)-*b*-PS are shown in Figure 6. The brush chains of grafted PEG are attached on the backbone chains crossing the adjacent PS layers. Consequently, dissolving the lower molecular weight PEG results in expansion of the backbone chains on which the PEG is grafted, while higher molecular weight PEG must be squeezed

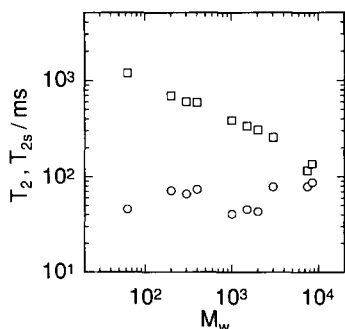


Figure 7 Spin-spin relaxation time of the tracer PEG against molecular weight (M_w) of the tracer PEG at 80°C: (○) T_2 in PS-*b*-P(S-*g*-PEG)-*b*-PS/PEG; (□) T_{2s} in pure melt

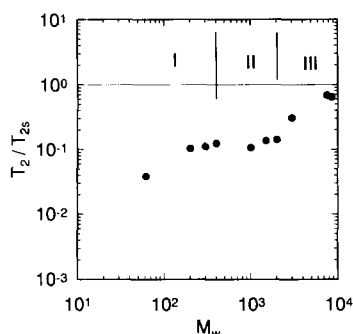


Figure 8 Ratio T_2/T_{2s} against molecular weight (M_w) of the tracer PEG for the tracer PEG in PS-*b*-P(S-*g*-PEG)-*b*-PS/PEG at 80°C: (I) regime I; (II) regime II; (III) regime III

out between the backbone chains, in a direction parallel to the layers. In the case of system 1 (diblock copolymer/homopolymer), the homopolymer of higher molecular weight is squeezed out in a direction perpendicular to the layers. Irrespective of this difference, the spatial distribution of the homopolymer tracer relative to the brushes of microstructured copolymer is essentially the same in both cases. Therefore, the diffusion behaviour is also very similar.

As seen above, the observed unique molecular weight dependence in the tracer diffusion of chain molecules dissolved in the microdomain is considered to be commonly observed in most microstructured block copolymer/tracer homopolymer systems. In conclusion, spatial distribution of the tracer can be the most dominant factor in controlling the tracer diffusion in the microphase domain.

In the following, three experimental facts will be given supporting the above explanation.

Change in relaxation time of segmental motions of tracer PEG on being confined in the microdomain

Since the protons of PEG are directly attached to the backbone chain, the T_2 of the proton nuclei must directly reflect segmental motions of the polymer chain²³. Figure 7 shows the relaxation time T_2 of the tracer PEG in the microstructured block copolymer and the relaxation time T_{2s} in the pure melt as functions of the molecular weight M_w of PEG. While T_{2s} decreases with increasing M_w monotonously, the change of T_2 with M_w is not monotonous. This is similar to the behaviour of the diffusion coefficients shown in Figure 4. However, T_2 and T_{2s} have much weaker dependences on M_w than

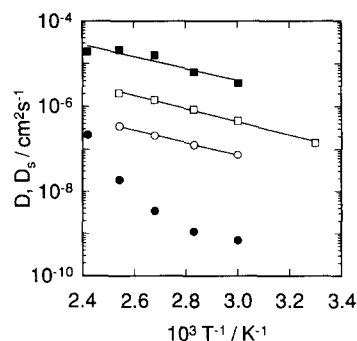


Figure 9 Semilogarithmic plots of D (or D_s) against $1/T$ for PEG (●, ○) in PS-*b*-P(S-*g*-PEG)-*b*-PS/PEG and (■, □) in pure melts. M_w : (●, ■) 62 (regime I) and (○, □) 400 (regime II). Apparent activation energy (kJ mol^{-1}): (■) 26.6, (□) 29.7 and (○) 28.2. The solid lines are linear least-squares fitting lines

D and D_{2s} , respectively, because the spin-spin relaxation time reflects the segmental motion which is less dependent on the chain length than the translational motion of the whole chain. To represent change in segmental motions of the tracer on being dissolved in the microdomain, the ratio T_2/T_{2s} is plotted against molecular weight of the tracer in Figure 8. Corresponding to Figure 5, one can see the three regimes. In regime I, the ratio T_2/T_{2s} increased with increasing molecular weight of the tracer, but the increment was very small compared with that of D/D_s . This fact implies that, in regime I, it is not the change of segmental mobility but the presence of the grafted chains as obstacles which is responsible for the slowing down of tracer diffusion in the microstructured matrix. In contrast to the results for regime I, T_2/T_{2s} in regime II is constant at $T_2/T_{2s} = 0.12$ independent of the molecular weight, and this is exactly the same as the behaviour of D/D_s , i.e. $(T_2/T_{2s}) \cong (D/D_s)$. Therefore, the reduction of the diffusion coefficient by confinement in the microdomain comes from depression of segmental motion in regime II. This also allows us to suppose that 'tortuosity' effects arising from the microphase structure are negligible. In regime III, where the homopolymer and the copolymer are considered immiscible, T_2/T_{2s} approaches unity as expected, similar to D/D_s .

The T_2 behaviour mentioned above is consistent with our explanation for the diffusion behaviour described earlier.

Temperature dependence of D and D_s of the PEG chains

Figure 9 shows the temperature dependence of the diffusion coefficient for a PEG tracer ($M_w = 62$) in regime I and a PEG tracer ($M_w = 400$) in regime II. No large difference in temperature dependence between D and D_s was found for the PEG with $M_w = 400$ in regime II. In this regime, the matrix may have indirect effects on the diffusion of homopolymer because of the localization of the spatial distribution of the tracer and, as a result, D and D_s have a similar temperature dependence*. On the contrary, in regime I, the tracer diffusion in the microphase shows a different temperature dependence from that in the pure melt. To illustrate this contrast more clearly, the ratio D/D_s was plotted against

*This is not in conflict with the change of T_2 (segmental relaxation time) in this regime, i.e. $T_2/T_{2s} \cong 0.12 \neq 1$, because the temperature dependence (or the apparent activation energy) is not always so sensitive to the change in mobility of segmental motions

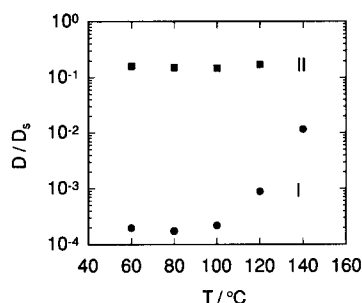


Figure 10 Temperature dependences of the ratio D/D_s for the tracer PEG in PS-*b*-P(S-*g*-PEG)-*b*-PS/PEG. M_w : (■) 62 (regime I); (●) 400 (regime II)

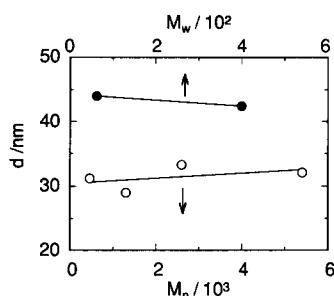


Figure 11 Molecular weight dependence of the long period (interdomain distance) d for (●) PS-*b*-P(S-*g*-PEG)-*b*-PS/PEG and (○) PS-*b*-PDMS/PDMS/ d_6 -Bz

temperature for regimes I and II in Figure 10. D/D_s in regime II started increasing sharply around 100°C with increasing temperature, while D/D_s in regime I was almost constant. Considering that the glass transition temperature of PS is $\sim 100^\circ\text{C}$, the tracer diffusion in regime I seems to be more directly affected by molecular motions of the matrix. This is expected from the spatial distribution of the tracer illustrated in Figure 6: above this temperature, the mobility of the molecular motions of the PS backbones with grafted PEG chains becomes higher owing to softening of the PS layers, which may directly induce an increase in the diffusion coefficient of the tracer PEG.

It should be noted here that the change in D with temperature shown in Figure 9 was reversible with increasing and decreasing temperature, so that no irreversible change in the microphase structure and no phase separation could be supposed.

Dependence of the long period of the microphase structures on the molecular weight of tracer polymers

Change in spatial segmental distribution with molecular weight of the homopolymer must produce dependence of the long period (interdomain distance) on the molecular weight. In the case of the diblock copolymer/homopolymer system, the long period increases with increasing molecular weight as observed

by Hashimoto *et al.*²². In the case of the present triblock copolymer, the long period may decrease with increasing molecular weight of the homopolymer, because the direction of the localization of the homopolymer against the microphase layer is different from those of ordinary diblock copolymer/homopolymer systems as already mentioned (cf. Figures 3 and 6).

Figure 11 shows the long period measured by SAXS against molecular weight of the homopolymer. A change in long period with molecular weight is so subtle that a definite conclusion cannot be deduced, but the results appear to show that the long period increases with molecular weight in PS-*b*-PDMS/PDMS/ d_6 -Bz, while it decreases in PS-*b*-P(S-*g*-PEG)-*b*-PS/PEG, in accordance with the above consideration.

ACKNOWLEDGEMENTS

This work was partly supported by Grant-in-Aid no. 01850196 from the Ministry of Education, Science and Culture of Japan. The PS-*b*-P(S-*g*-PEG)-PS was provided by the late Professor Fujimoto of Nagaoka University of Technology and Science.

REFERENCES

- Lodge, T. P., Rotstein, N. A. and Prager, S. in 'Advances in Chemical Physics' (Eds I. Prigogine and S. A. Rice), Vol. 79, Wiley, New York, 1990, p. 1
- Doi, M. and Edwards, S. F. 'The Theory of Polymer Dynamics', Clarendon Press, Oxford, 1986
- Bishop, M. T., Langlely, K. H. and Karasz, F. E. *Phys. Rev. Lett.* 1986, **57**, 1741
- Bishop, M. T., Langlely, K. H. and Karasz, F. E. *Macromolecules* 1989, **22**, 1220
- Guo, Y., Langlely, K. H. and Karasz, F. E. *Macromolecules* 1990, **23**, 2022
- Easwar, N., Langlely, K. H. and Karasz, F. E. *Macromolecules* 1990, **23**, 738
- Dozier, W. D., Drake, J. M. and Klafter, J. *Phys. Rev. Lett.* 1986, **56**, 197
- Brochard, F. *J. Phys.* 1977, **38**, 1285
- Brochard, F. and de Gennes, P. G. *J. Chem. Phys.* 1977, **67**, 52
- Davidson, M. G. and Deen, W. M. *J. Membrane Sci.* 1988, **35**, 167
- Muthukumar, M. and Baumgartner, A. *Macromolecules* 1989, **22**, 1937, 1941
- Guillot, G., Leger, L. and Rondlez, F. *Macromolecules* 1985, **18**, 2531
- Guillot, G. *Macromolecules* 1987, **20**, 2600, 2606
- Balsara, N. P., Eastman, C. E., Foster, M. D., Lodge, T. P. and Tirrell, M. *Makromol. Chem., Macromol. Symp.* 1991, **45**, 213
- Fredrickson, G. H. and Milner, S. T. *Mater. Res. Soc. Symp. Proc.* 1990, **177**, 169
- Isono, Y., Fujimoto, T. and Watanabe, O. *Polym. Prepr. Jpn* 1989, **38**, 1681
- Hahn, L. *Phys. Rev.* 1950, **80**, 580
- Carr, H. Y. and Purcell, E. M. *Phys. Rev.* 1954, **94**, 630
- Kubo, T. and Nose, T. *Polym. J.* 1992, **24**, 1351
- von Meerwall, E. and Kamat, M. *J. Magn. Reson.* 1989, **83**, 309
- Meiboom, S. and Gill, D. *Rev. Sci. Instrum.* 1958, **29**, 688
- Hashimoto, T., Tanaka, H. and Hasegawa, H. *Macromolecules* 1990, **23**, 4378
- Farrar, T. C. and Becher, E. D. 'Pulse and Fourier Transform NMR. Introduction to Theory and Methods', Academic Press, New York, 1971, Ch. 4